Online Recognition of Bimanual Coordination Provides Important Context for Movement Data in Bimanual Teleoperated Robots

Jacob R. Boehm[1], *Student Member IEEE*, Nicholas P. Fey[1], *Member IEEE*, Ann Majewicz Fey, *Member IEEE*[1,2]

***Abstract*— An important problem in designing human-robot systems is the integration of human intent and performance in the robotic control loop, especially in complex tasks. Bimanual coordination is a complex human behavior that is critical in many fine motor tasks, including robot-assisted surgery. To fully leverage the capabilities of the robot as an intelligent and assistive agent, online recognition of bimanual coordination could be important. Robotic assistance for a suturing task, for example, will be fundamentally different during phases when the suture is wrapped around the instrument (i.e., making a c-loop), than when the ends of the suture are pulled apart. In this study, we develop an online recognition method of bimanual coordination modes (i.e., the directions and symmetries of right and left hand movements) using geometric descriptors of hand motion. We (1) develop this framework based on ideal trajectories obtained during virtual 2D bimanual path following tasks performed by human subjects operating Geomagic Touch haptic devices, (2) test the offline recognition accuracy of bimanual direction and symmetry from human subject movement trials, and (3) evalaute how the framework can be used to characterize 3D trajectories of the da Vinci Surgical System's surgeon-side manipulators during bimanual surgical training tasks. In the human subject trials, our geometric bimanual movement classification accuracy was 92.3% for movement direction (i.e., hands moving together, parallel, or away) and 86.0% for symmetry (e.g., mirror or point symmetry). We also show that this approach can be used for online classification of different bimanual coordination modes during needle transfer, making a C loop, and suture pulling gestures on the da Vinci system, with results matching the expected modes. Finally, we discuss how these online estimates are sensitive to task environment factors and surgeon expertise, and thus inspire future work that could leverage adaptive control strategies to enhance user skill during robot-assisted surgery.**

I. INTRODUCTION

To fully capitalize on recent advances in robot sensing and control in teleoperated or wearable robotic systems, there is a critical need for effective methods to model the human as part of the collective co-robotic system. A key part of modeling a human operator is predicting operator intent and quantifying how the operator is using the system.

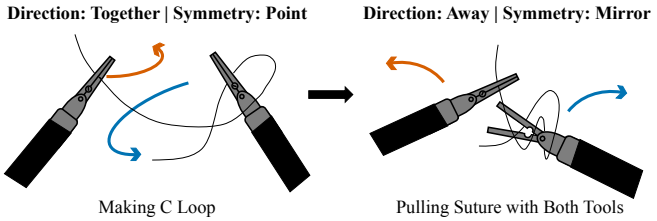

Fig. 1: Bimanual tasks, such as surgical knot tying, are composed of many distinct motions for each hand. For example, looping suture requires hands moving together with point symmetry, while pulling suture to form a knot requires hands moving apart in a mirrored fashion. Integrating recognition of these bimanual coordination modes could improve the design of assistive teleoperated robots.

Online prediction of these characteristics would enable new methods to enhance user performance during robot use. In addition, the use of robotic systems that are bimanual (i.e., allowing for the human to use both left and right hands to operate the system), pose a considerable challenge to filling this gap in knowledge. There are several important examples of bimanual robots including rehabilitation devices, such as exoskeletons and manipulandums, intended to enhance or retrain individuals to a level of motor function necessary for activities of daily living (ADL). Surgical robots also require highly complex bimanual skills to perform surgical tasks safely and effectively. Accurately modeling surgeon bimanual coordination in robotic surgery is critical for skill assessment and especially important when developing objective credentialing protocols (e.g., surgical residency programs, clinical adoption of new robotic techniques, etc.) [1]–[6].

In the literature, human movement for a task is often decomposed into subtasks, sometimes called gestures or "movemes". For example, in a drawing exercise, unimanual movements were segmented and classified into three movemes as reaching, drawing, or circling [7]. In another study, three different surgical tasks (knot tying, needle passing, and suturing) recorded in the JHU-ISI Gesture and Skill Assessment Working Set (JIGSAWS) were decomposed into 15 distinct gestures noted as "surgemes" [8]–[11]. These decomposition methods have been used to automate gesture recognition using predictive models like Continuous Hidden Markov Models, Gaussian Mixture Models, and various machine learning models [12]–[14]. With these predictive models, when a prior subtask is recognized, the current subtask can be more easily predicted and a device designer has the ability to provide augmented feedback to the user.

*This work was supported by the National Center for Advancing Translational Sciences of the National Institutes of Health under award Number UL1TR001105 and NSF #1846726.

[1]Jacob Boehm and Nicholas P. Fey are with the Walker Department of Mechanical Engineering, Cockrell School of Engineering, The University of Texas at Austin, Austin, TX 78712, USA Jacob.Boehm@austin.utexas.edu

[3]Ann Majewicz Fey is with the Walker Department of Mechanical Engineering, Cockrell School of Engineering, The University of Texas at Austin, Austin, TX 78712, USA and the Department of Surgery, University of Texas Southwestern Medical Center, Dallas, TX 75390, USA

There is a tremendous body of work devoted to the analysis of data for the purpose of skill evaluation as it relates to surgical tasks and gestures [15]. While the ability to reliably, automatically, and objectively evaluate skill is invaluable, many methods offer little to no analysis beyond a rating of skill. This is a caveat of what is sometimes referred to as a "black box" approach, especially when regarding machine learning methods. There has been a recent push to include information that would be meaningful for a trainee in order to improve performance. Such information could enhance training, feedback, and assistance if leveraged properly. One study highlights portions of a task that contribute most to the skill evaluation [16]. Another study uses semantic labels to quantify surgical style [17].

From a different perspective, researchers studying motor control have long produced studies with respect to assessing human movement [18], [19]. In the case of bimanual motion, many of these studies decompose movements into somewhat subjective spatio-temporal classifications [20]. This type of classification can be used across all bimanual tasks and is not dependent on the task performer. These studies have influenced many other studies on rehabilitation and athletics that seek to determine optimal training methods [21]. More recently, robotics, like upper limb exoskeletons, have been used to aid these training efforts [22], [23]. However, the ambiguity of definitions in prior literature and across disciplines hinders the advancement of tools for assessment and assistance of bimanual coordination training [20]. Also, no method for online recognition of spatial bimanual coordination modalities currently exists, to the best of our knowledge. Such a method is necessary to better design teleoperated robots for safe and effective bimanual control.

To bridge the gap between human movement and motor control fields of research and robotics, the purpose of our study was to 1) develop an online recognition method of bimanual coordination modes (i.e., bimanual direction and symmetry) using geometric descriptors based on cursor trajectories obtained during virtual 2D bimanual path following tasks completed by humans operating Geomagic Touch haptic devices, 2) test offline recognition accuracy of bimanual direction and symmetry during these trials, and 3) compare how the framework transfers to 3D trajectories of the da Vinci Surgical System's end-effectors during bimanual robot-assisted surgical-training tasks. These goals were performed to enable innovative robotic systems that are capable of providing online feedback to the human operator during a task. We feel an important contribution of the current study is the technique used for recognition of bimanual human movement using a geometric characterization that can be implemented in real-time in a bimanual robotic system to distinguish between a variety of specific coordination modes. As noted, While many options exist for the classification of bimanual movements, we focus on types of direction (i.e., hands moving together, in parallel, or away from each other), and types of symmetry (e.g., mirrored, point symmetry, not symmetric, etc.), and base this recognition purely on geometrical properties of left and right bimanual motion.

TABLE I: Notation for Recognition of Bimanual Coordination Modes

Notation	Definition
L, R	related to left or right hand, respectively
f	bimanual coordination metric
T	classification threshold
Dir	related to bimanual direction modality
Sym	related to bimanual symmetry modality
Mir	related to mirror symmetry
Pt	related to point symmetry
Vis	related to visual symmetry
τ_k	k^{th} time parameter of movement from 0 to 1
M	onset of classification prediction

II. METHODS

A. Definitions of Bimanual Coordination

Bimanual movements are discrete trajectories from one position to another involving both hands. These trajectories are described by two sets of ordered points in Cartesian space, one for left and right hand each.

$$X_L = \left\{(x_{l_1}, y_{l_1}, z_{l_1}), (x_{l_2}, y_{l_2}, z_{l_2}), ..., (x_{l_{n_l}}, y_{l_{n_l}}, z_{l_{n_l}})\right\}$$
$$X_R = \left\{(x_{r_1}, y_{r_1}, z_{r_1}), (x_{r_2}, y_{r_2}, z_{r_2}), ..., (x_{r_{n_r}}, y_{r_{n_r}}, z_{r_{n_r}})\right\} \quad (1)$$

Due to the variance in trajectory lengths and density of sampled points along trajectories of bimanual movements, paths must be normalized to ensure an unbiased analysis. We accomplish this by interpolating the sampled point sets to create equally spaced points p_{i_j} arranged as row vectors in matrices, C_L and C_R, of length, n.

$$C_i = \begin{bmatrix} p_{i_1} \\ p_{i_2} \\ \vdots \\ p_{i_n} \end{bmatrix}, i = L, R: \quad (2)$$

The choice of n and point spacing will affect the analysis of the movements, so they should be chosen based on workspace size, position sensor resolution, and number of sampled points. Using these normalized sets of ordered points, the segments of bimanual movements may further be analyzed using following characteristics.

1) Direction: Types of direction for a bimanual movement include moving together ($\rightarrow\leftarrow$), parallel ($\rightarrow\rightarrow$), or away ($\leftarrow\rightarrow$). The type of direction of a discrete bimanual movement can be distinguished by the Euclidean distance between successive points as denoted by f_{Dir}.

$$d_j = \left\| p_{l_j} - p_{r_j} \right\|_2 \quad (3)$$

$$f_{Dir_j} = d_j - d_{j-1} \quad (4)$$

If the Euclidean distance of successive points is monotonically decreasing, the direction is together; if it is monotonically increasing, the direction is away; and if the distance remains constant, the direction is parallel. Note that a movement may change direction during its execution.

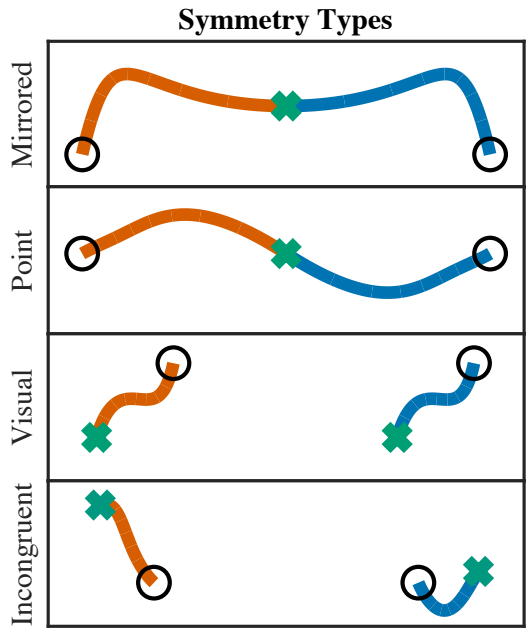

Fig. 2: Examples of types of symmetry of 2D bimanual movements, including mirrored, point, visual, and incongruent.

2) Symmetry: Symmetry of a bimanual movement may be described as mirror symmetric, point symmetric, visual symmetric, or incongruent (Fig. 2). Symmetry of bimanual movements requires point to point comparison of the right and left hand point sets because in the ideal cases of symmetry, one set of points can be equal to a scaled, translated, or rotated equivalent of the other set,

$$C_L = bC_RQ + v \tag{5}$$

In equation 5, b is a scaling factor, Q is an orthogonal reflection and rotation matrix, and v is a translational component. Types of symmetry are discerned by rotation and reflection component Q. Mirror symmetry is a Householder reflection, so $Q = I - 2qq^T$ where $\|q\| = 1$. Point symmetry is defined by a point reflection, $Q = -I$. Visual symmetry is simply a translation of one point set to another with no rotation, $Q = I$. Finally, incongruent bimanual movements are those such that no transformation described by Eqn. 5.

Combinations of types of direction and symmetry are referred to hereafter as bimanual motion modes. Particular bimanual motion modes are impossible due to definition constraints. This includes unit scaled movement with visual symmetry and direction type together or away. By definition,

$$C_L = C_R + v \tag{6}$$

therefore,

$$d_j = \left\|p_{l_j} - p_{r_j}\right\| = v \;\; \forall j \tag{7}$$

$$f_{Dir_j} = d_j - d_{j-1} = 0 \tag{8}$$

Thus, we can use the direction of a movement to help identify its symmetry.

B. Bimanual Coordination Recognition

1) Problem Statement: For the purposes of recognizing coordination in human movement data, we must consider a noisy version of the point matrices,

$$\widetilde{C}_i = C_i + w_i \tag{9}$$

where w_i is a noise matrix and C_i is the underlying movement with ideal direction and symmetry types. Due to the additive noise, evaluation of f_{Dir} requires a hysteresis band, $(-T_{Dir}, +T_{Dir})$, to discern the types of direction. The threshold T_{Dir} is chosen in accordance with the work space and number of sampled points. For sections or the entirety of a movement, the median of f_{Dir} is taken.

In order to predict types of symmetry of human bimanual movements, we use a modified Procrustes analysis. Procrustes analysis uses minimization techniques to determine the best transformation from one point set to another via the following equation [24].

$$\min_{b,Q,v} \left\|\widetilde{C}_L - b\widetilde{C}_RQ + v\right\|_F \tag{10}$$

Equation 10 may return any fitting orthogonal Q. However, we are interested in specific forms of symmetry, so our modified version limits Q to three options defined by the types of symmetry. Also, since our only concern is Q, we can reduce Eqn. 10 further.

$$\begin{aligned} f_{Sym} &= \min_{Q} \left\|\widetilde{C}_{0L} - \widetilde{C}_{0R}Q\right\|_F : \\ Q &= I, -I, I - 2qq^T \\ \|q\| &= 1 \end{aligned} \tag{11}$$

In the above, point sets have been normalized to be zero mean with a norm of one, i.e. $\|C_0\|_F = 1$. Equation 11 produces a scalar, which we label f_{Sym}, that may be thought of as a goodness-of-fit measure for the respective transformation. For ideal cases of symmetry, f_{Sym} is zero, and incongruent bimanual trajectories will have f_{Sym} with range $(0, 2]$. From this we can discern the type of symmetry from given movement data.

Due to the minimization, in non-ideal cases of bimanual symmetry as measured from human generated trajectories, f_{Sym} tends to be minimized with mirror symmetry ($Q = I - 2qq^T$) regardless of the underlying symmetry. We can model the problem as follows,

$$f_{Sym} = \min_{Q} \|C_{0L} - C_{0R}Q + w\|_F \tag{12}$$

where we have grouped the left and right noise terms, leaving underlying symmetric point matrices C_{0L} and C_{0R}. If the problem is split relative to the types of symmetry,

$$\begin{aligned} f_{Mir} &= \min_{q} \left\|\widetilde{C}_{0L} - \widetilde{C}_{0R}(I - 2qq^T)\right\|_F : \\ \|q\| &= 1 \end{aligned} \tag{13}$$

$$f_{Pt} = \left\|\widetilde{C}_{0R} + \widetilde{C}_{0L}\right\|_F \tag{14}$$

$$f_{Vis} = \left\|\widetilde{C}_{0R} - \widetilde{C}_{0L}\right\|_F \tag{15}$$

we can see that extracting the noise term from C_{0L}, C_{0R}, and minimization variable q in Eqn. 13 is not possible. Thus, the noise is included in computing a minimal f_{Mir}. If we assume that there exists underlying symmetry in $\widetilde{C}_{0L}$ and $\widetilde{C}_{0R}$, then Eqn. 13 can be reduced to

$$f_{Mir} = \sqrt{2 - 2tr(\widetilde{C}_{0L}^T \widetilde{C}_{0R}) + 4 \min_q q^T \widetilde{C}_{0L}^T \widetilde{C}_{0R} q} \quad (16)$$

The solution to Eqn. 16 becomes a well-known quadratic minimization problem with the solution related to the minimum eigenvalue of $\widetilde{C}_{0L}^T \widetilde{C}_{0R}$. For 2-dimensional point sets,

$$f_{Mir} = \sqrt{2(1 - \lambda_{max} + \lambda_{min})} \quad (17)$$

where λ_{max} and λ_{min} are the maximum and minimum eigenvalues of $\widetilde{C}_{0L}^T \widetilde{C}_{0R}$. As movements of non-mirror type symmetry become more linear, this measure diminishes, which becomes a problem when trying to distinguish between mirror symmetric movements and non-mirror symmetric movements. Therefore, we must filter out cases of point and visual symmetry first.

For movements that are not point symmetric, f_{Pt} tends toward 2. For example, take a visual symmetric movement with negligible noise, i.e. $C_{0L} = C_{0R}$.

$$f_{Pt} = \|2C_{0R}\|_F = 2\|C_{0R}\|_F = 2 \quad (18)$$

The same occurs for movements that tend away from an underlying visual symmetry and f_{Vis}. However, due to noise, we need to determine what the expected value of f_{Pt} and f_{Vis} are when the underlying symmetry is point and visual, respectively. By assuming the underlying symmetry is either point or visual, we can compute the expected value for f_{Pt} and f_{Vis} to be

$$E[f_{Sym}] = E[\|w\|_F] = E[\sqrt{trace(ww^T)}] \quad (19)$$

Assuming w is populated by i.i.d. zero-mean normal random variables with variance σ_w^2 means that f_{Sym} for underlying symmetry types point and visual is a Chi-distributed random variable with mean $\mu = \sigma_w \sqrt{2}\Gamma((np+1)/2)/\Gamma(np/2)$ and variance $\sigma^2 = \sigma_w^2 np - \mu^2$. Here, the mean and variance are dependent on the gamma function with degrees of freedom np, such that n is the number of points and p is the dimension. Over the course of a trajectory np grows to be quite large, so we can use Sterling's approximation to estimate the mean as

$$\mu \approx \sigma_w \sqrt{np-1}(1 - \frac{1}{4np}) \quad (20)$$

and the variance as

$$\sigma^2 \approx \sigma_w^2 \frac{(np-1)}{2np} \quad (21)$$

Just as with direction, we create thresholds, T_{Pt} and T_{Vis} to choose the classification. First, we normalize the symmetry metric by dividing by $\sqrt{np-1}(1 - \frac{1}{4np})$. Then, we choose thresholds based on the approximated mean and variance for samples of a given task.

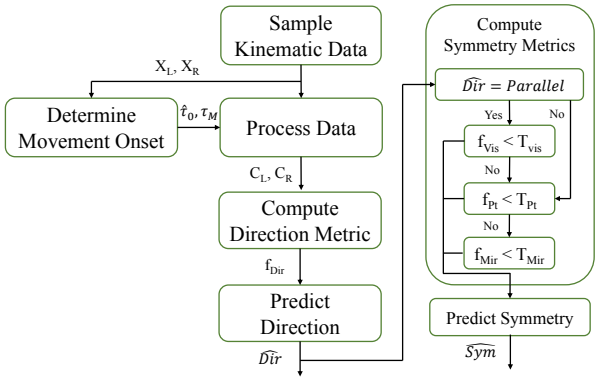

Fig. 3: Decision flow diagram for predicting bimanual coordination modes with respect to direction and symmetry.

After filtering out point and visual symmetries, we need to distinguish between mirror symmetric and incongruent movements. The expected value and variance for f_{Mir} assuming a mirrored movement are far more complex because of the minimization. Thus, it is more convenient to take a similar approach to that of point and visual symmetries. Therefore, we similarly normalize f_{Mir} by dimension and number of points and choose T_{Mir} from the mean and variation of a sample of movements.

2) Decision Flow: From the definitions, metrics, and subsequent properties of the proposed method, we can devise an sequence to optimally distinguish bimanual coordination modes (Fig. 3). First, sampled position data is parsed for movement onset. Then, it is filtered and sorted into equidistant point matrices. Point sets may also be centered and normalized at this time. Next, the metric for type of direction is computed, and the type of direction is estimated. Then, depending on the type of direction, symmetry metrics are computed. Finally, the type of symmetry is estimated based on the normalized symmetry metric.

Note that for this framework to be implemented online, a minimum of three sampled data points is required and the complexity is $O(p^3)$ due to the calculation of eigenvalues. If we limit p to a small number of dimensions, as is often the case, the complexity becomes $O(n)$. For reasonable values of n, modern systems are capable of computing these metrics in near-real time.

C. Experimental Data

The data used for validation in this study consists of 1150 unique trajectories from a 2D data set as recorded during a bimanual path following experiment that includes 11 subjects [25]. Subjects followed pre-determined paths generated in accordance to the different types of bimanual movement coordination modes. Position data were recorded at 500 Hz. For this set, used a moving average filter with window of 0.05 seconds. In this set there is an ideal path (objective ground truth) from which we can determine noise variance σ_w and choose optimal thresholds. Trials with f_{Sym} greater than three scaled median absolute deviation from the

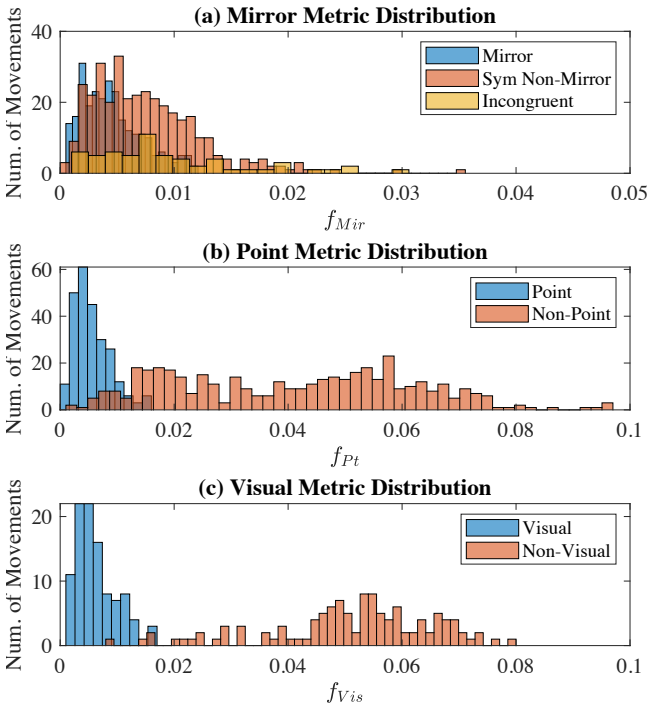

Fig. 4: Distribution of f_{Sym} as computed from movements of the 2D bimanual path following task split such that movements with the true underlying symmetry are grouped in blue bins. (a) demonstrates how movements with underlying point and visual symmetry need to be tested for first because the calculation of f_{Mir} for all symmetry types is minimized so they become indistinguishable. In (b) and (c) there is clear distinction between movements with underlying point and visual symmetry and other symmetries or incongruent movements for f_{Pt} and f_{Vis}.

median of trials with the same ground truth symmetry were removed as outliers. Trials with ground truth incongruent symmetry such that the ideal trajectory had f_{Sym} less than the chosen symmetry thresholds were also removed. The direction threshold band for this set was chosen as $T_{Dir} = \pm 0.15mm$. Symmetry thresholds were chosen as $T_{Mir} = 0.0096$, $T_{Pt} = 0.00125$ of, and $T_{Mir} = 0.00141$. These thresholds were chosen using statistical methods. Accuracy was calculated on a per trial basis comparing the predicted bimanual coordination mode to the ground truth of the ideal trajectory.

We used a second 3D data set to prove the applicability and importance of this method. This data set is known as JIGSAWS, and which includes examples of 3 realistic surgical gestures, transferring needle $(n = 173)$, making C loop $(n = 53)$, and pulling suture $(n = 61)$, from 8 subjects [10], [11]. Gestures were grouped to analyze their relation to bimanual motion modes. Each segment of a gesture was trimmed and split automatically into instances of bimanual motion using a precise movement onset detection method [26]. Only bimanual movements where both hands were moving simultaneously were included. This set's position data were recorded at 30 Hz. For this set, we tuned the moving average filter window to 0.1 seconds and T_{Dir} to

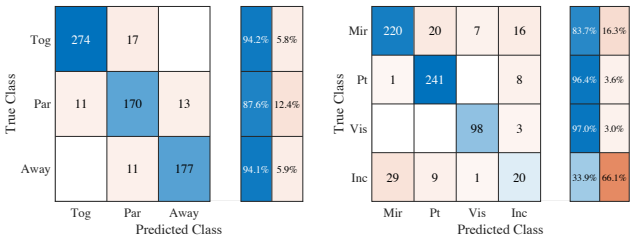

(a) Direction Confusion Matrix (b) Symmetry Confusion Matrix

Fig. 5: Confusion matrices for bimanual coordination mode prediction of (a) direction and (b) symmetry types as compared to ground truth trajectories, post-movement of 2D bimanual path following trials.

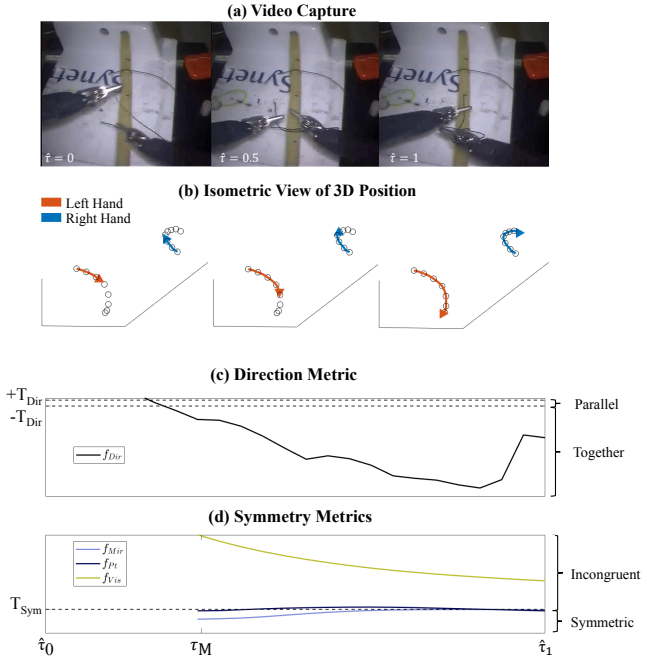

Fig. 6: Bimanual coordination mode recognition for an instance of making a C loop with (a) video capture, (b) 3 dimensional position plots of the left and right hand, and (c) direction, f_{Dir}, and (d) symmetry metrics, f_{Mir}, f_{Pt}, and f_{Vis} computed over parametrized time of the movment. This example has a bimanual coordination mode of direction type together and point symmetry.

± 0.1 mm. The symmetry thresholds were set at $T_{Sym} = T_{Mir} = T_{Pt} = T_{Vis} = 0.06$. These thresholds were chosen through generalization of the 2D case to 3D and hand tuning, however, the mathematical framework did not change. Generalization was done by normalizing the computed symmetry metrics with respect to number of points and dimension, as noted previously. Hand tuning was done by viewing the distributions, similar to Fig. 4, for samples of select gestures. This is a recognized limitation of this study.

III. RESULTS

For the 2D path following task, trials took a mean time of 1.501 seconds and a median time of 1.418 seconds to complete. Computed symmetry metrics yielded distributions

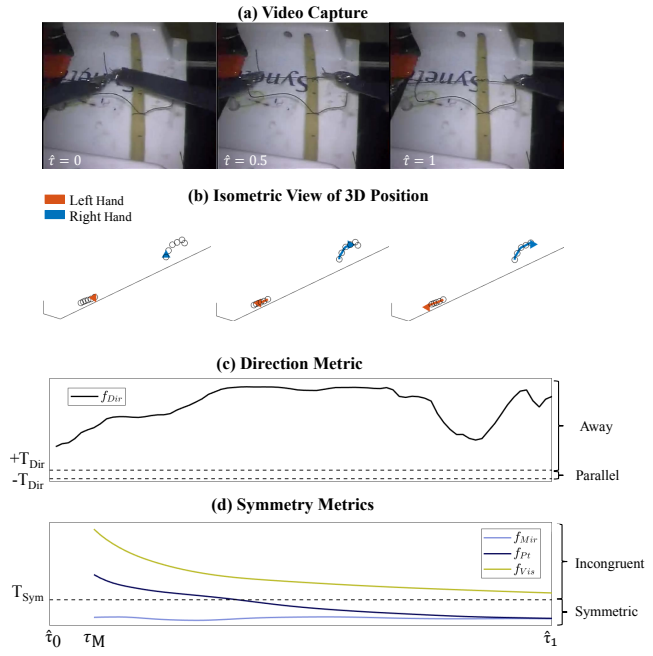

Fig. 7: Bimanual coordination mode recognition for an instance of suture pulling with (a) video capture, (b) 3 dimensional position plots of the left and right hand, and (c) direction, f_{Dir}, and (d) symmetry metrics, f_{Mir}, f_{Pt}, and f_{Vis} computed over parametrized time of the movment. This example has a bimanual coordination mode of direction type away and starts as mirror symmetry then changes to point symmetry.

of f_{Sym} as shown in Fig. 4. Mean and standard deviation after normalization for f_{Mir} was 0.00458 and 0.00268, for f_{Pt} was 0.0056 and 0.00317, and for f_{Vis} was 0.00632 and 0.00351, respectively. Using f_{Pt} and f_{Vis}, we determined the approximate standard deviation of noise, σ_w, to be 0.006 for this task. The overall recognition accuracy for direction was 92.3% with individual accuracies of 94.2% for together, 87.6% for parallel, and 94.1% for away (Fig. 5 (a)). The overall accuracy for symmetry was 86.0% (Fig. 5 (b)). Individual types of symmetry were recognized with accuracies of 83.7% for mirror, 96.4% for point, 97.0% for visual, and 33.9% for incongruent.

For the 3D surgical robotic tasks, the predicted bimanual motion modes of completed movements of surgical gestures are summarized in Table II. The majority of transferring needle movements have bimanual coordination mode with direction of together and mirror symmetry (50%). Many others have symmetry type incongruent (20%) or point (15%). The majority of making C loop movements have direction together with symmetry type mirror (34%) or incongruent (31%). Only 12% of making C loop gestures had symmetry type point. For pulling suture movements, the majority have bimanual coordination mode away and point (46%) or mirror symmetry (23%). Bimanual coordination modes of surgical movements were able to be predicted within 250 milliseconds.

IV. DISCUSSION

The purpose of this study was to develop an online recognition method of bimanual coordination modes (i.e., bimanual direction and symmetry) using geometric descriptors of left and right upper limb motion. We developed this framework based on trajectories obtained during virtual 2D bimanual path following tasks completed by humans operating haptic devices. We tested the offline recognition accuracy of bimanual direction and symmetry during these trials, and compared how the framework transfers to 3D trajectories of the da Vinci Surgical System's surgeon-side manipulators during bimanual surgical training tasks. The recognition method presented in this study had high accuracy for all direction types and symmetric bimanual movements. Note that these accuracies indicate the statistical significance of computed metrics (Fig. 4) for this data set. The confusion of recognizing incongruent movements that we observed in the 2D tasks could be attributed to movement coupling. Humans have a natural tendency to couple their movements, so the actual measured movements may have deviated from the incongruent ground truth trajectories to trajectories that were symmetric [27], [28].

Our results which showed how classifying bimanual motion during robot-assisted surgical taks were found to be fairly intuitive regarding the predicted bimanual directions. To transfer a needle or make a c loop, one needs to bring the hands together. Pulling a suture involves the hands moving away to tighten the suturing thread. Surprisingly, very few movements during "making a c loop" gestures had point symmetry. In order to make the loop, one has to wrap thread with one tool in a spiral motion around the other. We suggest the discrepancy here may be due to two reasons. The first is that the spiraling wrap may be captured better in the rotation of the wrists than in the position data. Second, the majority of the beginning of the movement may be point symmetric, but finished as incongruent, and we have reported the predictions for the fully completed movement.

Another important consideration is that each gesture contains variability regarding bimanual coordination modes. Some movements of needle transfer and suture pulling are also parallel. Some of this variability comes from extraneous movements made during a gesture that were picked up by the movement detection method that we used. Such extraneous movements may also be indicative of perfomance during the task. However, the variability in bimanual coordination modes may also be attributed to the environment. We expected to see most suture pulling movements to be mirror symmetric, but more were point symmetric. From Fig. 6 (a) and 7 (a), we can see that there is a tube blocking the right tool from pulling the thread in a mirror symmetric fashion. Operators adapted their movements to go over this tube, thereby making the movement point symmetric. This is evidence that there are different bimanual coordination modes used to accomplish the same gestures. A closer look at the correlation of task performance and bimanual coordination modes has the potential to improve our understanding of how

TABLE II: Surgical Task Bimanual Analysis Results

Surgical Gesture	**Transfering Needle**			**Making C Loop**			**Pulling Suture**		
	Together	Parallel	Away	Together	Parallel	Away	Together	Parallel	Away
Mirror	94	9	7	20	3	3	15	1	19
Point	28	2	0	3	3	1	1	0	39
Visual	0	0	0	0	0	0	0	3	0
Incongruent	38	4	6	18	5	2	3	1	2

a task may best be performed.

For trials that were correctly classified in the 2D bimanual path following data set, the time to predict the movements' bimanual coordination mode (on the order of hundreds of milliseconds) compared to the time of movement was short enough that the prediction could be integrated into the control of a robotic system. We suggest the most important benefit of this study is the ability to predict coordination as it evolves over time. Movements may change direction or symmetry type as they are performed, as indicated by Fig. 6 and Fig. 7. Our proposed and tested method would allow for the visualization and integration of those changes in a robotic system, which if leveraged properly may improve performance. One method to do so would be in the form of haptic force feedback. For teleoperated systems such as the da Vinci Surigcal System, there exists an opportunity to push users toward skillful types of coordination that are found in expert users, or to push them away from idealized trajectories through error amplification so that users can learn to be skillful in more challenging environments.

There are a few limitations of this study, such as the exclusion of other characterizations of bimanual movement that could also be important, depending on a given application. These include the number of targets, scaling, sequence, and temporal classifications (e.g. phase of cyclical motions) of bimanual motion [20], [29]. In addition, the selection of the thresholds when generalizing the method to different tasks requires some manual tuning using statistical methods dependent on the task and sampled set. One explanation of this result is that different tasks could require different noise characterizations. Another explanation is that overfitting of the first data set may have contributed to difficulty in generalizing. A study involving physical neuroscience methods that look at processes and activation of the brain during bimanual motion may help in determining appropriate thresholds for labeling movements, especially with regards to symmetry. We suggest observing the effects of performing movements with varying degrees of symmetry and direction (i.e., varying f_{Sym}) on cognitive processes would be beneficial, as done similarly in a prior study [30].

V. CONCLUSION AND FUTURE WORK

In this paper, we demonstrate ability to recognize bimanual coordination modes from human movement trajectories using purely geometric features. This development may well integrate with the control system of a co-robotic systems, such as an upper-limb rehabilitation or surgical robots, for augmenting performance due to a fast computation time. We have also shown the variablity of movements in realistic tasks as related to bimanual coordination modes, thus noting the importance of this kind of classification in bimanual movement analysis, especially as it relates to surgical skill assessment. We believe that this study has the potential to impact how humans are modeled in human-machine systems, particularly those that can provide feedback, as well as how human bimanual motions are modeled in general. We also expect that this approach will facilitate the opportunity to provide meaningful feedback with sufficient temporal resolution.

In future work, we intend to explore automated methods for tuning thresholds in the method presented in this paper so that it is more easily applicable across tasks. We also plan to incorporate other classifications of bimanual movement, such as number of targets, scaling, and sequence, and look at various forms of feedback during movement to observe how it affects training of fine, bimanual motor skills.

REFERENCES

[1] M. A. Thornby and D. E. Krebs, "Bimanual skill development in pediatric below-elbow amputation: a multicenter, cross-sectional study," *Archives of Physical Medicine and Rehabilitation*, vol. 73, pp. 697–702, 1992.

[2] G. Lewis and E. Perreault, "An assessment of robot-assisted bimanual movements on upper limb motor coordination following stroke," *IEEE Transactions on Neural Systems and Rehabilitation Engineering*, vol. 17, pp. 595–604, 2009.

[3] G. Herrnstadt, N. Alavi, B. Randhawa, L. A. Boyd, and C. Menon, "Bimanual elbow robotic orthoses: preliminary investigations on an impairment force-feedback rehabilitation method," *Frontiers in Human Neuroscience*, vol. 9, no. 169, 2015.

[4] C. Wu, C. Yang, M. Chen, K. Lin, and L. Wu, "Unilateral versus bilateral robot-assisted rehabilitation on arm-trunk control and functions post stroke: a randomized controlled trial," *Journal of NeuroEngineering and Rehabilitation*, vol. 10, 2013.

[5] O. van der Meijden and M. P. Schijven, "The value of haptic feedback in conventional and robot-assisted minimal invasive surgery and virtual reality training: a current review," *Surgical Endoscopy*, vol. 23, no. 6, pp. 1180–1190, 2009.

[6] H. Abboudi, M. S. Khan, O. Aboumarzouk, K. A. Guru, B. Challacombe, P. Dasgupta, and K. Ahmed, "Current status of validation for robotic surgery simulators–a systematic review," *BJU international*, vol. 111, no. 2, pp. 194–205, 2013.

[7] D. Del Vecchio, R. M. Murray, and P. Perona, "Decomposition of human motion into dynamics-based primitives with application to drawing tasks," *Automatica*, vol. 39, no. 12, pp. 2085–2098, 2003.

[8] C. E. Reiley and G. D. Hager, "Task versus subtask surgical skill evaluation of robotic minimally invasive surgery," in *International conference on medical image computing and computer-assisted intervention*. Springer, 2009, pp. 435–442.

[9] H. C. Lin, *Structure in surgical motion*. The Johns Hopkins University, 2010.

[10] Y. Gao, S. S. Vedula, C. E. Reiley, N. Ahmidi, B. Varadarajan, H. C. Lin, L. Tao, L. Zappella, B. Béjar, D. D. Yuh *et al.*, "Jhu-isi gesture and skill assessment working set (jigsaws): A surgical activity dataset for human motion modeling," in *MICCAI Workshop: M2CAI*, vol. 3, 2014, p. 3.

[11] N. Ahmidi, L. Tao, S. Sefati, Y. Gao, C. Lea, B. B. Haro, L. Zappella, S. Khudanpur, R. Vidal, and G. D. Hager, "A dataset and benchmarks for segmentation and recognition of gestures in robotic surgery," *IEEE Transactions on Biomedical Engineering*, vol. 64, no. 9, pp. 2025–2041, 2017.

[12] M. Power, H. Rafii-Tari, C. Bergeles, V. Vitiello, and G.-Z. Yang, "A cooperative control framework for haptic guidance of bimanual surgical tasks based on learning from demonstration," in *2015 IEEE International Conference on Robotics and Automation (ICRA)*. IEEE, 2015, pp. 5330–5337.

[13] C. E. Reiley, E. Plaku, and G. D. Hager, "Motion generation of robotic surgical tasks: Learning from expert demonstrations," in *2010 Annual international conference of the IEEE engineering in medicine and biology*. IEEE, 2010, pp. 967–970.

[14] M. M. Rahman, N. Sanchez-Tamayo, G. Gonzalez, M. Agarwal, V. Aggarwal, R. M. Voyles, Y. Xue, and J. Wachs, "Transferring dexterous surgical skill knowledge between robots for semi-autonomous teleoperation," in *2019 28th IEEE International Conference on Robot and Human Interactive Communication (RO-MAN)*. IEEE, 2019, pp. 1–6.

[15] C. E. Reiley, H. C. Lin, D. D. Yuh, and G. D. Hager, "Review of methods for objective surgical skill evaluation," *Surgical endoscopy*, vol. 25, no. 2, pp. 356–366, 2011.

[16] H. I. Fawaz, G. Forestier, J. Weber, L. Idoumghar, and P.-A. Muller, "Accurate and interpretable evaluation of surgical skills from kinematic data using fully convolutional neural networks," *International journal of computer assisted radiology and surgery*, vol. 14, no. 9, pp. 1611–1617, 2019.

[17] M. Ershad, R. Rege, and A. M. Fey, "Automatic and near real-time stylistic behavior assessment in robotic surgery," *International journal of computer assisted radiology and surgery*, vol. 14, no. 4, pp. 635–643, 2019.

[18] C. M. Hughes, B. Mäueler, H. Tepper, and C. Seegelke, "Interlimb coordination during a cooperative bimanual object manipulation task," *Laterality: Asymmetries of Body, Brain and Cognition*, vol. 18, no. 6, pp. 693–709, 2013.

[29] J. R. Boehm, N. P. Fey, and A. Majewicz-Fey, "Effects of scaling and sequence on performance of dynamic bimanual path following tasks," *Journal of Medical Robotics Research*, 2020.

[19] P. J. Bryden, "The influence of mp bryden's work on lateralization of motor skill: Is the preferred hand selected for and better at tasks requiring a high degree of skill?" *Laterality: Asymmetries of Body, Brain and Cognition*, vol. 21, no. 4-6, pp. 312–328, 2016.

[20] C. Shirota, J. Jansa, J. Diaz, S. Balasubramanian, S. Mazzoleni, N. A. Borghese, and A. Melendez-Calderon, "On the assessment of coordination between upper extremities: towards a common language between rehabilitation engineers, clinicians and neuroscientists," *Journal of neuroengineering and rehabilitation*, vol. 13, no. 1, p. 80, 2016.

[21] A. Utley, *Motor Control, Learning and Development: Instant Notes*. Routledge, 2018.

[22] B. Kim and A. D. Deshpande, "An upper-body rehabilitation exoskeleton harmony with an anatomical shoulder mechanism: Design, modeling, control, and performance evaluation," *The International Journal of Robotics Research*, vol. 36, no. 4, pp. 414–435, 2017.

[23] E. D. Oña, J. M. Garcia-Haro, A. Jardón, and C. Balaguer, "Robotics in health care: Perspectives of robot-aided interventions in clinical practice for rehabilitation of upper limbs," *Applied sciences*, vol. 9, no. 13, p. 2586, 2019.

[24] J. C. Gower, G. B. Dijksterhuis *et al.*, *Procrustes problems*. Oxford University Press on Demand, 2004, vol. 30.

[25] J. R. Boehm, N. P. Fey, and A. Majewicz-Fey, "Inherent kinematic features of dynamic bimanual path following tasks," *IEEE Transactions of Human Machine Systems*, 2020.

[26] G. H. Staude, "Precise onset detection of human motor responses using a whitening filter and the log-likelihood-ratio test," *IEEE transactions on biomedical engineering*, vol. 48, no. 11, pp. 1292–1305, 2001.

[27] R. Sleimen-Malkoun, J.-J. Temprado, L. Thefenne, and E. Berton, "Bimanual training in stroke: How do coupling and symmetry-breaking matter?" *BMC neurology*, vol. 11, no. 1, p. 11, 2011.

[28] S. P. Swinnen, V. Puttemans, S. Vangheluwe, N. Wenderoth, O. Levin, and N. Dounskaia, "Directional interference during bimanual coordination: is interlimb coupling mediated by afferent or efferent processes," *Behavioural Brain Research*, vol. 139, no. 1-2, pp. 177–195, 2003.

[30] G. W. Goerres, M. Samuel, I. H. Jenkins, and D. J. Brooks, "Cerebral control of unimanual and bimanual movements: an h215o pet study," *Neuroreport*, vol. 9, no. 16, pp. 3631–3638, 1998.